Modern Physics Letters B
2150007 (15 pages)

DOI: 10.1142/S021798492150007X

A novel dissipative and conservative megastable oscillator with engineering applications

Karthikeyan Rajagopal*, Jay Prakash Singh†, Akif Akgul‡,¶, Anitha Karthikeyan*,
Prakash Duraisamy§, Binoy Krishna Roy† and Ahmet Karaca‡

*Nonlinear Systems and Applications,
Faculty of Electrical and Electronics Engineering,
Ton Duc Thang University, Ho Chi Minh City, Vietnam

†Control and Industrial Automation (C&IA) Group,
Department of Electrical Engineering,
National Institute of Technology (NIT) Silchar, Assam, India

‡Department of Electrical and Electronic Engineering, Faculty of Technology,
Sakarya University of Applied Sciences, Sakarya, Turkey

§Center for Nonlinear Dynamics, Institute of Research and
Development Defence University, Ethiopia

¶aakgul@sakarya.edu.tr; akgulakif@ieee.org

Received 19 March 2020
Revised 22 June 2020
Accepted 1 July 2020
Published 21 September 2020

In this paper, we have proposed a new chaotic megastable oscillator which has both conservative and dissipative characters depending on the selection of parameters. Various dynamical characteristics including megastability of the new system are investigated and presented. The bifurcation plots and the corresponding Lyapunov exponents (LEs) confirm the existence of both dissipative and conservative oscillations in the system. The proposed megastable oscillator is used as a carrier generator in a differential chaos shift keying (DCSK). Another application of the new chaotic oscillator is shown by using it in developing a random number generator (RNG) and the NIST test results are presented to show the statistical complexity of the new system.

Keywords: Chaos; chaotic systems; megastable oscillator; bifurcation; DCSK; RNG.

1. Introduction

The exploration of nonlinear oscillators is a significant milestone in the development of theories of dynamical systems. During an experimental study,[1] Van der Pol and Van der Mark considered the nonlinearity in a simple electronic circuit and found peculiar behavior (later named as "Chaos"). In 1945, Cartwright and Littlewood[2] identified a similar behavior in a nonlinear oscillator and documented it as a noisy structure with a determined pattern. The work of Lorenz's[3] revealed the deterministic nature of the behavior and portrayed the first known "Chaotic attractor".

Nonlinear dynamical systems have various responses starting from different initial conditions. Fixed points are those points where the solution does not change in time. The occurrence of more than one attractor in a nonlinear dynamical system and switching between one another for a change in the initial condition is defined as "Multistability". Such behavior is noted while investigating the dynamic behavior of various systems.[4–11] In Ref. 12, Li and Sprott investigated the classic Lorenz's system with unusual parameter values (negative and zero) and new-fangled attractors were captured. Additionally, the co-existence of limit cycles and strange attractors were identified. After the study of multistability, its popularity picked up among the researchers.[6–8] Many chaotic systems were developed so far with multistability which is found very useful in various fields including neuroscience,[?] laser optics,[4] reaction-diffusion systems,[13] etc.

Initially, multistability property is recognized with symmetric systems because the system equations remain unchanged to sign change of the variables.[6,12,14] Symmetric systems generally have symmetric pairs of the coexisting attractors, including equilibrium points, limit cycles, and strange attractors. Some asymmetric systems are also reported with multistability.[15–17] Recently, many chaotic systems were reported with multistability which will be useful in various fields of application.[6,7,9–11] Sprott *et al.*[18] extracted a type of multistability that holds a countable number of infinite coexisting attractors and named "Megastability". A temporally-periodic forcing function is added with the classic Vander-Pol oscillator, and the coexistence of countable infinity nested attractors is captured. Similarly, some more papers are available in the literature that exhibits "Megastability" using periodically forced function with nonlinear oscillators.[19–22] These megastable oscillators provide a platform to generate complex system which posses a variety of properties. In Ref. 23, quasiperiodic excitation function was included to get "megastable attractors". A quasiperiodic force term is introduced in a conservative and dissipative chaotic system and observed a countable infinity of nested coexisting attractors.[24] The characteristics of megastable oscillators can be easily modified and can be chosen by selecting the parameter values and initial conditions. Applications which require complex nature and sensitive characteristics can be modeled with megastable oscillators. Since the megastable oscillators can provide infinitely countable attractors, we can easily alter the system behavior based on the situation (Parameter values, initial condition, variation in excitation).

From the literatures, we could observe that most of the megastable attractors, the unforced systems do not exhibit chaos but will show multiple coexisting periodic limit cycles; however, by forcing the attractor with an external excitation, we can achieve multiple coexisting chaotic attractors depending on the chosen initial conditions. But such systems found least importance in applications such as Neuron modeling, secure communication, and random number generations. Thus, a question raises in our minds. "Is external excitation, a mandatory criterion to impinge the property "Megastability" into a nonlinear oscillator?" This curiosity motivated us to propose an unforced nonlinear oscillator that possesses both conservative and dissipative natures for different parameter values along with "Megastability".

In this paper, we proposed an unforced nonlinear megastable oscillator which posses dissipative and conservative based on the parameter selection. Complete dynamical analysis is carried out and numerical simulations are presented. In order to show the significance of parameter variation and its effects on the behavior of the system, we generated bifurcation diagrams with the corresponding Lyapunov spectrum. In Sec. 3, a potential application of the proposed megastable oscillator is discussed for differential chaos shift keying (DCSK). In Sec. 4, we show how efficient the system can be used in Random Number Generator (RNG) application.

2. Unforced Megastable Oscillator (UMO)

Chaotic oscillators with infinitely coexisting attractors have been of interest in recent years[19,25,26] and most of them have infinite number of equilibrium points. Some oscillators have finite equilibrium points and still exhibit infinitely the coexisting attractors; such oscillators are termed as "Megastable".[18] All those megastable oscillators discussed in the literature are forced with an external excitation to show chaotic attractors.[20,23,24,27] Hence, we are interested in proposing a new megastable oscillator which can show infinitely coexisting chaotic attractors without external excitation. The proposed system is derived from the modified Rossler system[28] by replacing $(y - y^2)$ term by $\sin(y)$ and adding state feedbacks to the third and fourth state equations. The new unforced megastable oscillator (UMO) is defined as

$$
\begin{aligned}
\frac{dx}{dt} &= -y - z \\
\frac{dy}{dt} &= x - w \\
\frac{dz}{dt} &= -a\sin(y) - bz \\
\frac{dv}{dt} &= cy - dv
\end{aligned}
\tag{1}
$$

where a, b, c, d are the system parameters. The Jacobian matrix of the UMO system is given as follows:

$$
\begin{bmatrix}
0 & -1 & -1 & 0 \\
1 & 0 & 0 & -1 \\
0 & -a\cos(y) & -b & 0 \\
0 & c & 0 & -d
\end{bmatrix}
\tag{2}
$$

The equilibrium points of the system are derived from two different cases. In the first case, we consider $d = 0$ and the UMO system shows a line equilibria on the $x = w$ line. In the second case, we consider $b = 0$ and the system shows infinite equilibrium points given by $\left(\frac{cn\pi}{d}, n\pi, -n\pi, \frac{cn\pi}{d}\right)$. The parameter value of a and c is

Table 1. Dissipative and conservative UMO.

Parameter values	Lyapunov exponents (LEs)	Sum of the LEs	Nature of the system
$b = 0$	$L_1 = 0.035$		
$d = 0.01$	$L_2 = 0$		
	$L_4 = -0.035$	-0.01	Dissipative
	$L_4 = -0.035$		
$b = 0.0001$	$L_1 = 0.016$	0	Conservative
$d = 0$	$L_2 = 0$		
	$L_3 = 0$		
	$L_4 = -0.016$		

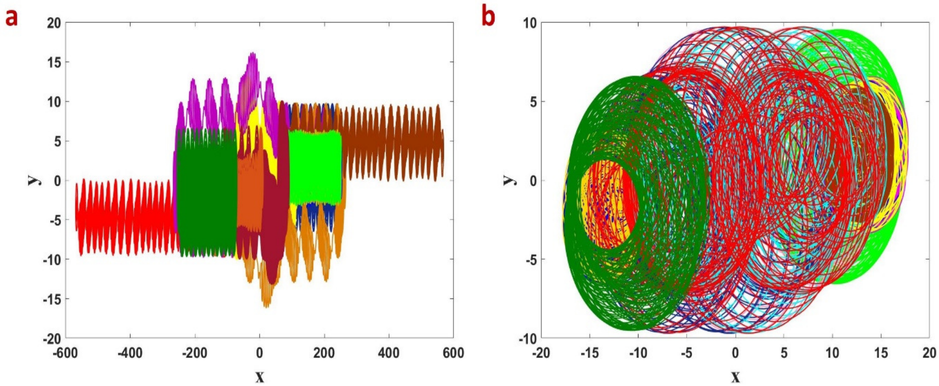

Fig. 1. (Color online) Phase portrait of the UMO for 10 initial conditions located on the x-axis (from $x = -5$ to $x = +5$ with steps equal to 1 for the dissipative system, shown in (a) and 10 initial conditions located on the x-axis (from $x = -1$ to $x = +1$ with steps equal to 0.1 for the conservative system, shown in (b) while the initial conditions of other states are kept to 0.

taken as 0.5 and 0.08, respectively. For Case-1, the eigenvalues of the UMO system are $\lambda_1 = 0.4025$; $\lambda_{2,3} = -0.2013 \pm 1.0960i$; $\lambda_4 = 0$ with $b = 0.0001$. For Case-2 (with $d = 0.01$), the characteristic polynomial of the UMO is given by

$$\lambda^4 + 0.01\lambda^3 + 1.08\lambda^2 - (0.5\cos(n\pi) - 0.01)\lambda - 0.005\cos(n\pi) \tag{3}$$

Depending on the values of the parameters b and d, the UMO system shows both conservative and dissipative natures, as shown in Table 1.

The phase portraits of the UMO for both the dissipative and conservative natures are shown in Fig. 1.

The dynamical behavior of the UMO is investigated using the bifurcation plots. We have done the bifurcation analysis of the UMO with the variation of a parameter and also of initial conditions. By fixing $d = 0$, we have derived the bifurcation of the UMO with parameter b as shown in Fig. 2(a). In Fig. 2(b), we have plotted

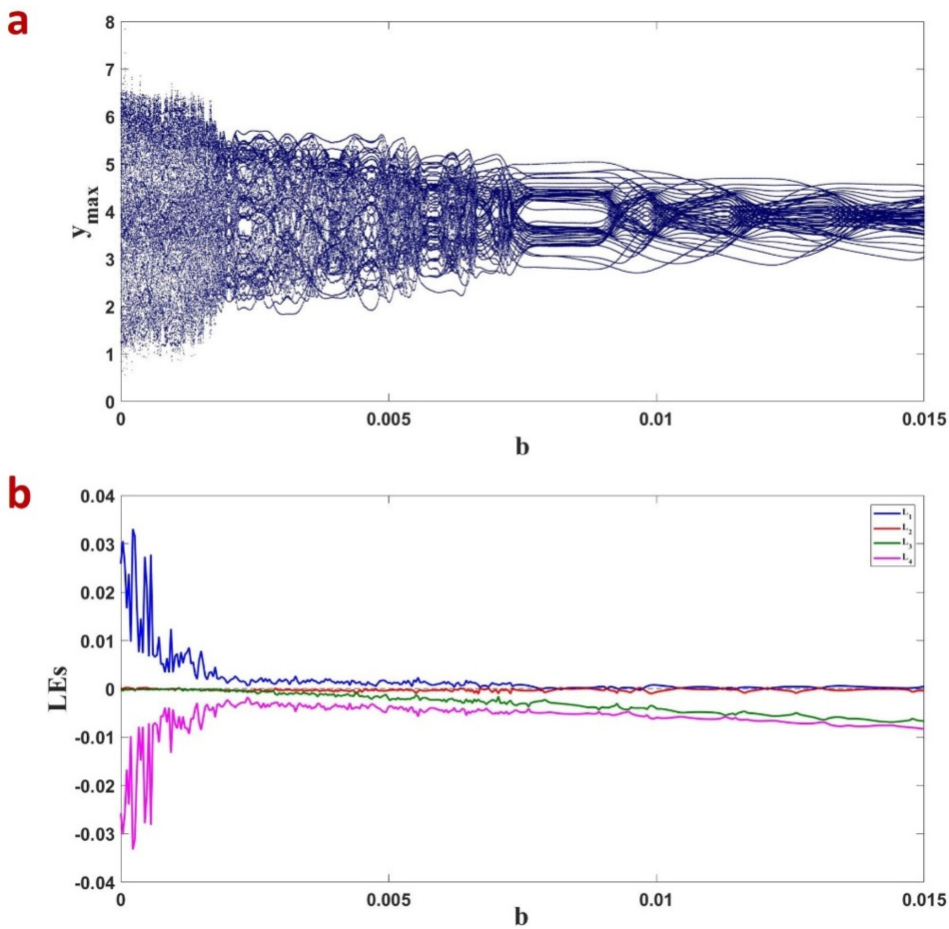

Fig. 2. (Color online) (a) Bifurcation of the UMO with parameter b for $d = 0$; (b) the corresponding LEs.

the respective finite time LEs. For $0 \leq b < 0.002$, the system shows a conservative chaotic attractor as seen from Fig. 2(b) and for $0.002 \leq b \leq 0.007$, the system shows a dissipative chaotic attractor.

In the next investigation, we consider the parameter $d = 0.01$ and derive the bifurcation of the UMO with parameter b. The system shows a dissipative chaotic attractor for $0 \leq b < 0.009$, as shown in Figs. 3(a) and 3(b).

To understand the importance of parameter d we have plotted the bifurcation of the UMO with the variation of d as shown in Fig. 4(a). For $0 \leq d \leq 0.15$, we see chaotic regions and the same can be confirmed with the respective LEs plotted in Fig. 4(b). Especially, for $0 \leq d < 0.05$ the UMO system shows dissipative chaotic attractor and for $0.05 \leq d \leq 0.15$, it shows conservative chaotic attractor.

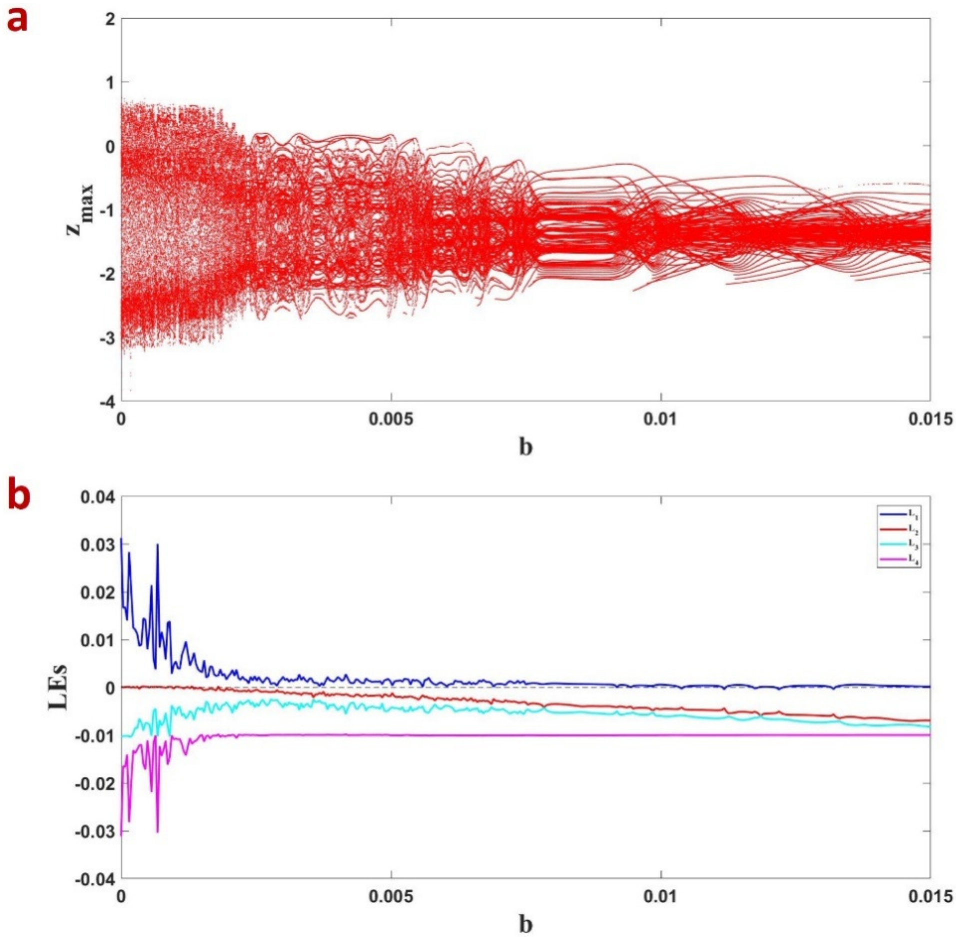

Fig. 3. (Color online) (a) Bifurcation of the UMO with parameter b for $d = 0.01$; (b) the corresponding LEs.

As the UMO is a megastable system, the importance of the role played by the initial conditions is also investigated. We have considered the initial condition of y z w is and derive the bifurcation of the system with x_0. In Fig. 5(a), we have considered $b = 0$ and $d = 0$ and the initial condition of the state x is varied from -5 to 5. For the entire region from $-5 \leq x_0 \leq 5$, the system shows conservative attractor which can be verified by the corresponding LEs, as shown in Fig. 5(b).

In our next discussion about the bifurcation of the UMO with initial conditions, we consider $b = 0$ and $d = 0.01$ and derive the bifurcation of the system with x_0 as shown in Fig. 6(a). It can be easily verified that the UMO system shows dissipative chaotic attractor for $-5 \leq x_0 \leq 5$ as seen from the respective LEs plots in Fig. 6(b).

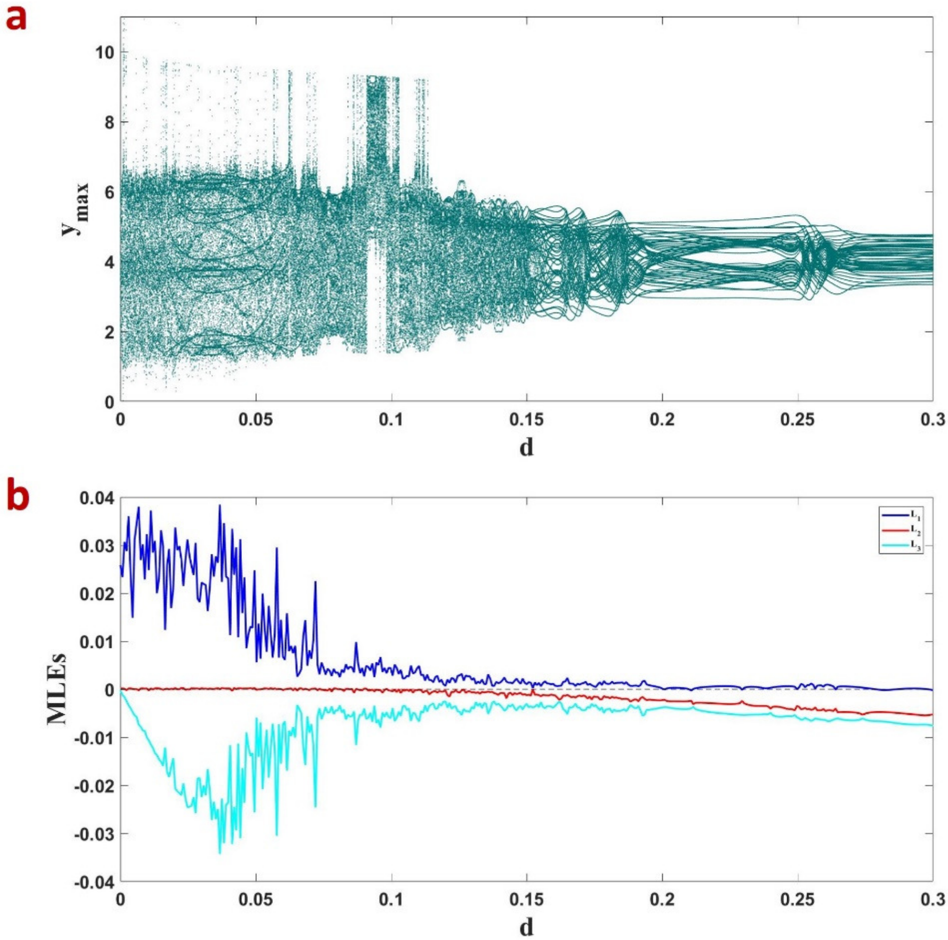

Fig. 4. (Color online) (a) Bifurcation of the UMO with parameter d for $b = 0$; (b) the corresponding LEs.

3. A Potential Application of the New System in DCSK

In this section, a potential application of the proposed system is discussed for DCSK.

3.1. *Principle of DCSK*

A periodic signal is commonly used as a transmission carrier in communication systems. This signal has a relatively narrow bandwidth after being modulated.[29] It is expected that such type of carrier signals may be degraded during the transmission through the multipath channel.

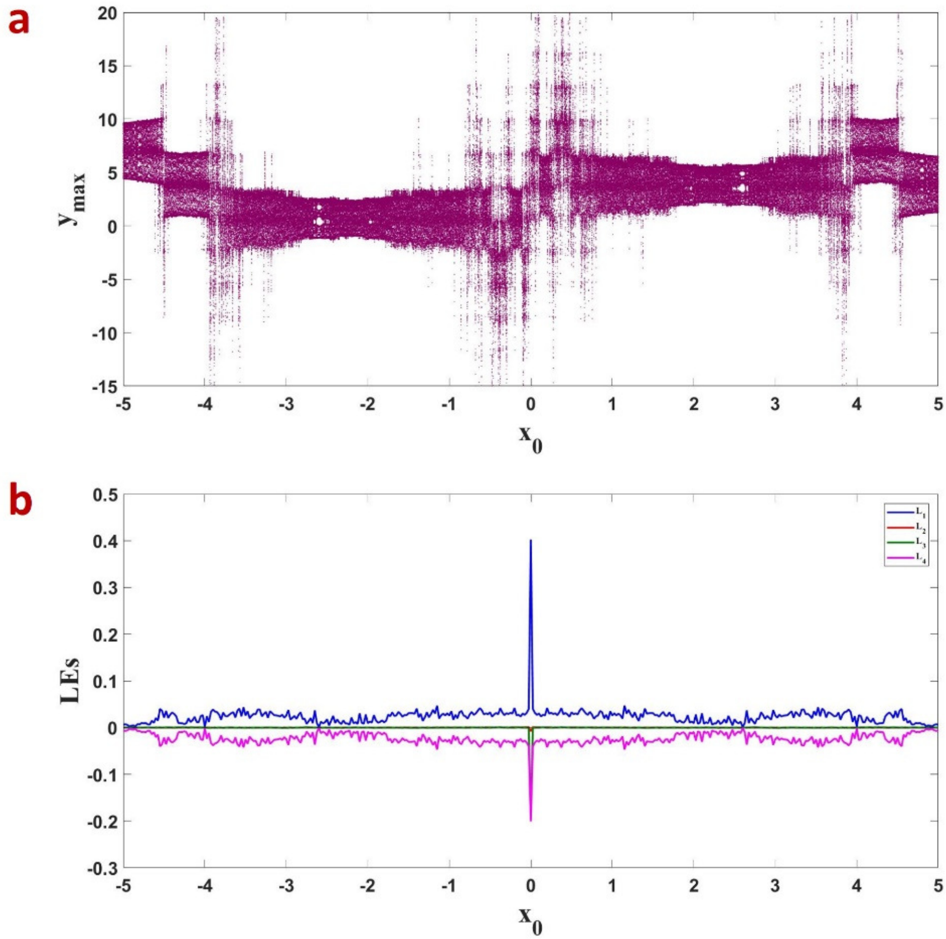

Fig. 5. (Color online) (a) Bifurcation of the UMO with initial condition x_0 and other initial conditions are taken as and parameters $b = 0$ and $d = 0$; (b) the corresponding LEs.

A chaotic signal produced by a nonlinear system has a broadband noise-like power spectrum and has good statistical properties. Chaotic signal has a noise-like autocorrelation waveform. This helps in good rejection of multipath fading. The chaotic signal has negligible cross-correlation that helps to better suppress the interference from the other users.[29] It is easy to generate in real-life. Another interesting feature is the high sensitivity to the initial condition. It is difficult to be deciphered. Therefore, the applications of a chaotic signal in communication become interesting.

The primary work in chaos shift keying was reported by Parlith and Dedieu in 1993.[30] In their work, the chaotic signal was used as an information carrier. During that time, the demodulation method was coherent demodulation. Coherent demodulation uses chaotic signal as a transmitter to send the binary (or hex) digital

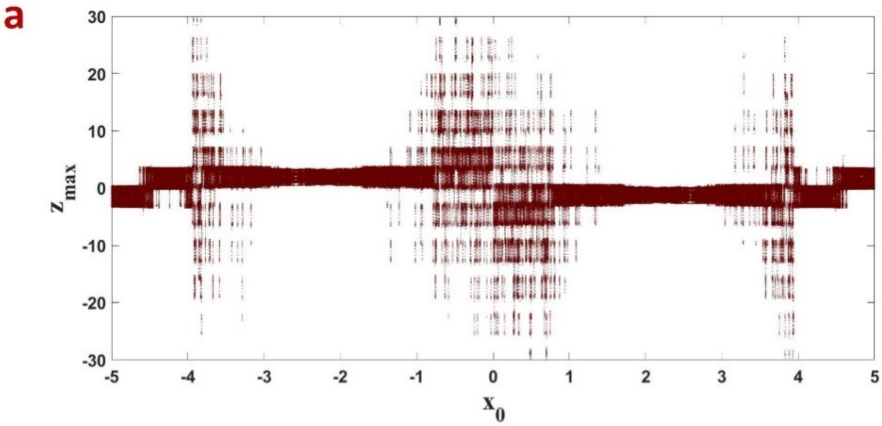

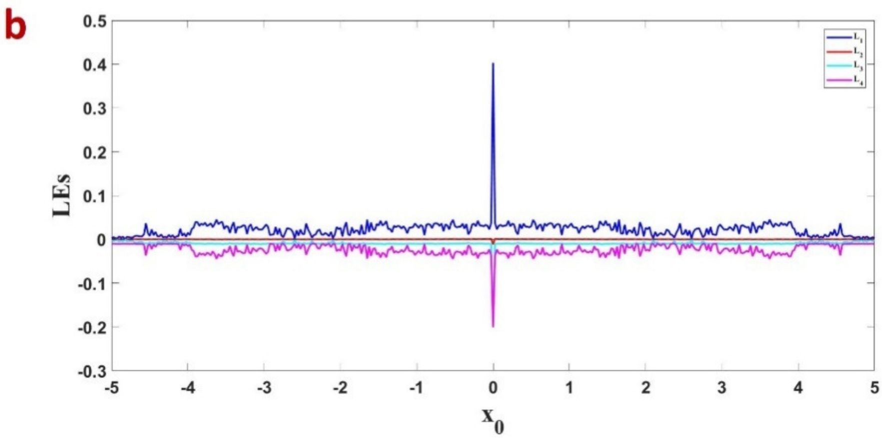

Fig. 6. (a) Bifurcation of the UMO with initial condition x_0 and other initial conditions are taken as and parameters $b = 0$ and $d = 0.01$; (b) the corresponding LEs.

information using a chaos shift keying. This is done by synchronizing the sending and receiving end chaotic signals by synchronization method based on one-way coupling and demodulate the signal at the receiving end. Practically, the chaotic synchronization is complex and costly.

Another method that overcomes the defects of the above, a DCSK was proposed by Kolumban in 1996.[30] Figure 7 shows the process of DCSK.[31–34]

It is seen from Fig. 7 that the signal of the chaotic system is used to transmit the information signal. Based on the above explanation, a chaotic signal is used as a carrier in DSCK for the following reasons:

(1) It is difficult to be deciphered.
(2) Good rejection of multipath fading.
(3) Better suppress the interference from the other users.
(4) It is easy to generate in real-life.

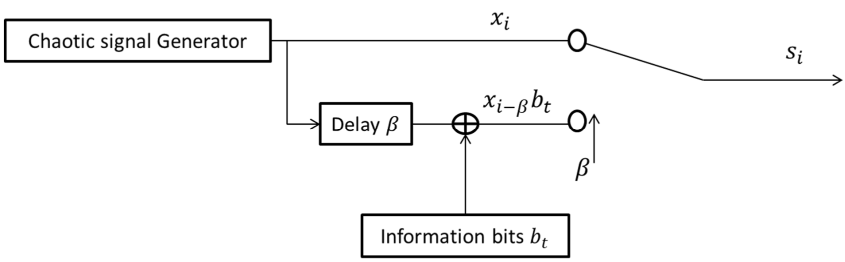

Fig. 7. DCSK modulation technique.

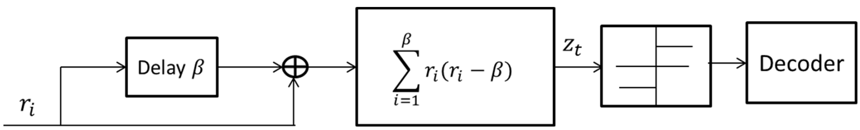

Fig. 8. DCSK demodulation technique.

In this technique, two-time slots are used for every bit. Chaotic sequence transmission, as a reference, is done in the first time-slot. The second time-slot is used for sending another chaotic signal to be used as a reference, having the same length as that in the first time-slot. The second time-slot is used as a reference. If the information signal and the reference signal are the same then the value of the information bit is +1. If the information signal is negative of the reference signal then the value of the information bit is −1. The expression of a signal at time t for bits b_k is given by

$$\begin{cases} x_i & 1 < i \leq \beta\,, \\ b_t x_{i-\beta} & \beta < i \leq 2\beta\,, \end{cases}$$

where β is the number of sampling points.

In Fig. 8, demodulation case, where the correlation between the received signal r_i and the delayed signal $r_{i-\beta}$ is done. The output of the correlator after time t is given by

$$z_t = \sum_{i=1}^{\beta} (r_i)(r_{i-\beta})\,.$$

The restored bit (b_t) is obtained as

$$\hat{b}_t = \mathrm{sgn}[z_t]\,.$$

The chaotic signal used as a carrier in the above DCSK has a random number like signal/bit. The randomness of the bits is proved and validated using the standard statistical tests. This requires the complete description of the generation and validation of a RNG using the proposed chaotic system. Section 4 discusses the RNG and its statistical test using the proposed system.

4. RNG Using the Proposed Chaotic System

It is known that chaotic systems are unpredictable and have random-like behavior. Such natures of chaotic systems are suitable for a RNG. Some applications like encryption, decryption of images or signals are done using an RNG. Various papers are available on the applications of chaotic system-based RNGs.[35–51,53,54] It is observed from the literature that most of the chaotic systems used for RNGs are chaotic maps. Only limited numbers of continuous-time chaotic systems are used as an RNG.[35–45] It is also observed that a few papers have shown the effectiveness and security analysis of the generated random number using the standard internationally accepted randomness test like FIPS-140-1 and NITS-800-22. Motivated with the above-status in the literature, here, the new continuous-time chaotic system is used to show its application in an RNG.

The following process is carried out to use the proposed system for the random number generation. Since the proposed chaotic system is a continuous-time dynamical system, the discretization process is carried out to use it in the random number generation. Chaotic systems are very sensitive to initial conditions and the numbers generated using them are random. Here, floating point numbers are generated from the proposed chaotic system by using the Runge–Kutta fourth-order algorithm. Table 2 shows the sampled floating-point numbers generated from the proposed system and their corresponding binary version. We consider a set of binary numbers which is the most complicated set. If the considered set of binary numbers satisfies the RNG test/statistical test, then such a set of binary numbers is termed as the most complicated set. But, for the RNG test/statistical test, a very large amount of binary numbers are to be generated. For example, the number of bits should be in the range 10,000–200,000. The most trusted and commonly used tests for an RNG are the FIPS-140-1 test[51] and the NIST-800-22 test.[52] The FIPS-140-1 test requires 20,000 bits and the NIST-800-22 test requires a minimum of 100,000 numbers for the better result. To know the performance of the generated random numbers using the proposed system, the internationally standard NIST-800-22 test is used here.

Table 2. The floating-point number and binary number generated from the proposed chaotic system.

Serial No.	Numerical outcomes	Transformation to a binary value
1	0.108325913612001	000110111011101100111111010000000
2	0.108958019990783	000110111110010010101100001111100
3	0.109594267464085	000111000000111001011110101100010
4	0.121786886477246	000111110010110101101100111001100
5	0.122507221551773	001110010011000101110001110111101
6	0.123232281147370	001110011110100100111111000100000
7	0.223410717326336	010011100111100011000111001011100
8	0.224808247172077	010011110111110010110001011010100
9	0.226215306751362	011011001100010100010010111000100
10	0.424882107133949	011011100011100101100111000100110

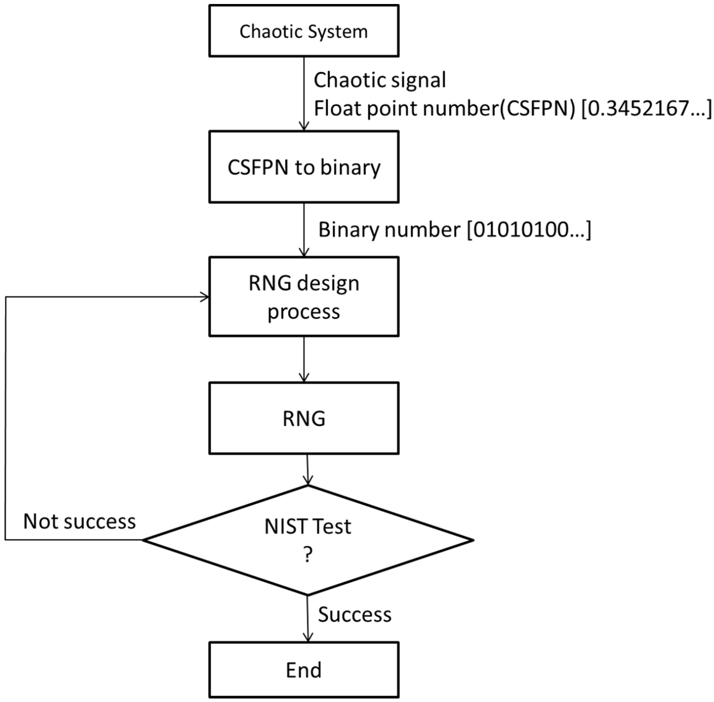

Fig. 9. Flow chart for generating a random number using a chaotic system.

It is apparent from Table 2 that the most significant bits have a similar pattern, but the least significant bits have fewer similarity patterns. It suggests that the use of the least significant bit of the generated random numbers may be more appropriate for the NIST statistical test. If the result is not successful, the randomness can be increased by using logical operations between the numbers like AND, OR and XOR, or by changing the bit's positions. It may be noted that the RNG using the proposed system passed the NIST-800-22 test. The complete flow chart for a RNG using a chaotic system is shown in Fig. 9.

The steps the RNG design process are as follows:

(1) Table 2 (please refer paper) shows sampled floating-point numbers generated from the proposed system and their corresponding binary numbers.
(2) It may be observed from Table 2 (please refer paper) that the most significant bits have similar patterns, but the least significant bits have fewer similar patterns. It suggests that the use of the least significant bits for the generation of the random numbers may be more appropriate.
(3) If the generated random numbers do not pass the NIST statistical tests, the randomness may be increased by using logical operations between the generated random numbers like AND, OR and XOR, or by choosing a different bit's position.

(4) We consider a set of binary numbers which is the most complicated set. The set of binary numbers that satisfy the standard statistical tests are termed as the most complicated set and qualify as a random number sequence.

The results of the NIST-800-22 statistical test for the RNG of the proposed system are given in Table 3. The results reveal that the designed RNG is successful since the obtained p-values are more than 0.001. Thus, the proposed system can be used as a carrier signal bit in DCSK and provide high data security.

Table 3. Random number generation (RNG)*NIST-800-22 tests of the proposed system in (1).

Statistical tests	p-values	Outcomes of the result
Frequency (Monobit) test	00.520495	Positive
Block-frequency test	0.0462	Positive
Cumulative-sums test	00.4165	Positive
Runs test	00.4641	Positive
Longest-run test	00.7176	Positive
Binary matrix rank test	00.7419	Positive
Discrete Fourier transform test	00.0516	Positive
Non-overlapping templates test	00.0121	Positive
Overlapping templates test	00.4867	Positive
Maurer's universal statistical test	00.3715	Positive
Approximate entropy test	00.1634	Positive
Random excursions test	00.5025	Positive
Random excursions variant test	00.6803	Positive
Serial test-1	00.5654	Positive
Serial test-2	00.0165	Positive
Linear-complexity test	00.4732	Positive

The energy distribution of x and y states of System (1) is depicted in Fig. 10. If a chaotic sequence has a more probability density of bit energy, it will give good performance in the application of a bit error ratio.[31–34]

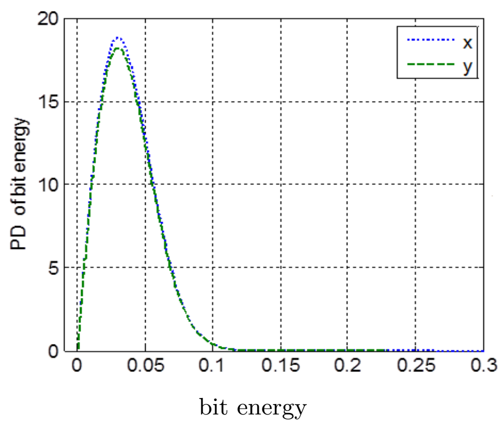

Fig. 10. Energy distribution of signals x and y of System (1).

5. Conclusion

A new megastable chaotic oscillator which exhibits both dissipative and conservative oscillations for different values of parameters is presented in this paper. The proposed chaotic oscillator exhibits megastability without a forcing function. Various analyses of the system like equilibrium points, LEs, bifurcation diagrams and Lyapunov spectrum are presented to show the complex behavior of the system. A DCSK modulation using the proposed megastable oscillator as the carrier generator is investigated and presented. Also, a RNG using the new megastable oscillator is presented and the complexity of the random number is investigated using the NIST tests. The simulation results confirm the claimed properties of the new chaotic oscillator.

References

1. B. Van der Pol and J. Van der Mark, *Nature* **120** (1927) 363.
2. M. L. Cartwright and J. E. Littlewood, *J. Lond. Math Soc.* **20** (1945) 180.
3. E. N. J. Lorenz, *Atmos. Sci.* **20** (1963) 130.
4. M. Brambilla, L. A. Lugiato and V. Penna, *Phys. Rev. A* **43** (1991) 5114.
5. F. Prengel, A. Wacker and E. Schöll, *Phys. Rev. B* **50** (1994) 1705.
6. Q. Lai and S. Chen, *Optik* **127** (2016) 3000.
7. K. Rajagopal, S. Jafari, A. Akgul and A. Karthikeyan, *Nonlinear Dyn.* (*Springer*) **93** (2018) 1087, doi:10.1007/s11071-018-4247-5.
8. K. Rajagopal, V. T. Pham, F. E. Alsaadi, F. E. Alsaadi, A. Karthikeyan and P. Duraisamy, *Eur. Phys. J.-Spec. Top.* 2018.
9. K. Rajagopal, P. Duraisamy, R. Weldegiorgis and A. Karthikeyan, *Shock Vib.* **2018** (2018) 1092812, doi:10.1155/2018/1092812.
10. Q. Lai, X.-W. Zhao, K. Rajagopal, G. Xu, A. Akgul and E. Guleryuz, *Pramana-J. Phys.* **90** (2018) 6, doi:10.1007/s12043-017-1493-x.
11. J. P. Singh, K. Lochan, N. V. Kuznetsov and B. K. Roy, *Nonlinear Dyn.* **90**(2) (2017) 1277.
12. C. Li and J. C. Sprott, *Int. J. Bifurcation Chaos* **23** (2013) 1350199.
13. P. Marmillot, M. Kaufman and J.-F. Hervagault, *J. Chem. Phys.* **95** (1991) 1206.
14. S. Schiff, K. Jerger, D. H. Duong, T. Chang, M. L. Spano and W. L. Ditto, *Nature* **370** (1994) 615.
15. B. Bao, Q. Li, N. Wang and Q. Xu, *Chaos* **26** (2016) 043111.
16. R. Barrio, F. Blesa and S. Serrano, *Physica D* **238** (2009) 1087.
17. C. Li and J. C. Sprott, *Optik* **127** (2016) 10389.
18. C. Li, J. C. Sprott and H. Xing, *Nonlinear Dyn.* **87** (2017) 1351.
19. J. C. Sprott, S. Jafari, A. J. M. Khalaf and T. Kapitaniak, *Eur. Phys. J. Spec. Top.* **226** (2017) 1979.
20. C. Li and J. C. Sprott, *Phys. Lett. A* **382**(8) (2018) 581.
21. H. Jahanshahi, K. Rajagopal, A. Akgul, N. N. Sari, H. Namazi and S. Jafari, *Int. J. Non-Linear Mech.* **107** (2018) 126.
22. F. Yuan, G. Wang and X. Wang, *Chaos* **26** (2016) 073107.
23. Z. Wang, H. R. Abdolmohammadi, F. E. Alsaadi, T. Hayat and V.-T. Pham, *Chaos Solitons Fractals* **110** (2018) 252.
24. K. Rajagopal, J. P. Singh, B. K. Roy and A. Karthikeyan, *Chin. J. Phys.* **58** (2019) 263.

25. P. Prakash, K. Rajagopal, J. P. Singh and B. K. Roy, *AEU-Int. J. Electron. Commun.* **92** (2018) 111.
26. C. Li, J. C. Sprott, W. Hu and Y. Xu, *Int. J. Bifurcation Chaos* **27**(10) (2017) 1750160.
27. C. Li, J. C. Sprott and Y. Mei, *Nonlinear Dyn.* **89**(4) (2017) 2629.
28. P. Prakash, K. Rajagopal, J. P. Singh and B. K. Roy, *Int. J. Bifurcation Chaos* **28**(9) (2018) 1830030.
29. P. S. Jay and B. K. Roy, *Nonlinear Dyn.* **89** (2017) 1845.
30. Z. Liu, J. Zhang and H. Liu, *Comput. Model. New Technol.* **18**(12C) (2014) 138, doi:10.1109/ISOCC.2012.6406912.
31. M. P. Kennedy and M. Hasler, *IEEE Trans. Circuits Syst. II: Analog Digit. Signal Process.* **40**(10) (1993) 634, doi:10.1109/82.246164.
32. N. Al Bassam and O. Jerew, *J. Comput. Networks Commun.* **2016** (2016).
33. N. Al Bassam, M. Bashir and E. P. Sumesh, An efficient DCSK?: A real time simulation for future chaotic communications, *2016 3rd MEC Int. Conf. Big Data and Smart City*, 15–16 March 2016, Muscat, Oman (IEEE, 2016), pp. 1–5, doi:10.1109/ICBDSC.2016.7460335.
34. M. N. Majeed, *J. Am. Sci.* **10**(10) (2014) 240.
35. G. Kaddoum, F. Richardson and F. Gagnon, *IEEE Trans. Communications* **61**(8) (2013) 3281 doi:10.1109/TCOMM.2013.071013.130225.
36. G. Kolumban, B. Vizvari, W. Scharz and A. Abel, Differential chaos shift keying?: A robust coding for chaos communication, in *Proc. Int. Workshop Nonlinear Dynamics of Electronic Systems*, August 1996, pp. 87–92.
37. L. G. de la Fraga, E. Torres-Pérez, E. Tlelo-Cuautle and C. Mancillas-López, *Nonlinear Dyn.* **90**(3) (2017) 1661.
38. I. Cicek, A. Emre and G. Dundar, *Integr. VLSI J.* **47**(1) (2013) 38.
39. E. Avaroglu, *Turk. J. Elec. Eng. Comp. Sci.* **25** (2017) 633.
40. L. L. Bonilla, M. Alvaro and M. Carretero, *J. Math. Ind.* **2017** (2017) 1.
41. I. Ozturk and R. Kihc, *Nonlinear Dyn.* **80**(3) (2015) 1147.
42. İ. Öztürk and R. Kiliç, *Int. J. Bifurcation Chaos* **24**(9) (2014) 1450107.
43. H. Zhu, C. Zhao, X. Zhang and L. Yang, *Comput. Secur.* **36** (2013) 40.
44. M. Francois, T. Grosges, D. Barchiesi and R. Erra, *Informatica* **24**(2) (2013) 181.
45. P. Wieczorek and K. Golofit, *IEEE Trans. Circuits Syst.* **61**(1) (2014) 134.
46. S. Coşkun, İ. Pehlİvan, A. Akgül and B. Gürevin, *Turk. J. Elec. Eng. Comp. Sci.* **27** (2019) 847.
47. K. Demir and S. Ergiin, *Entropy* **957**(20) (2018) 1.
48. A. Akgul, I. Moroz, I. Pehlivan and S. Vaidyanathan, *Optik* **127**(3) (2016) 5491.
49. A. Akgul, H. Calgan, I. Koyuncu, I. Pehlivan and A. Istanbullu, *Nonlinear Dyn.* **84**(2) (2015) 481.
50. R. Yeni, S. Kilinc and M. E. Yalcin, *Int. J. Bifurcation Chaos* **25**(2) (2015) 1550021.
51. M. E. Yalçın, J. A. K. Suykens and J. Vandewalle, *IEEE Trans. Circuits Syst. Regul. Papers* **51**(7) (2004) 1395.
52. F. Sun and S. Liu, *Chaos Solitons Fractals* **41**(5) (2009) 2216.
53. A. Rukhin *et al.*, A statistical test suite for random and pseudorandom number generators for cryptographic applications, NIST, April 2010.
54. A. Akgül, C. Arslan and B. Arıcıoğlu, *Chaos Theory Appl.* **1**(1) (2019) 1.
55. J. S. Teh, A. Samsudin, M. Al-Mazrooie and A. Akhavan, *Nonlinear Dyn.* **82**(4) (2015) 1913.